

PNEUMATICALLY-POWERED ROBOTIC EXERCISE DEVICE TO INDUCE A SPECIFIC FORCE PROFILE IN TARGET LOWER EXTREMITY MUSCLES

Gregory C. Henderson and Jun Ueda*

The G. W. Woodruff School of Mechanical Engineering, Georgia Institute of Technology, 771 Ferst Drive, Atlanta, GA, 30332-0405, USA

*corresponding author jun.ueda@me.gatech.edu

Summary

The goal of this research is to establish a methodology to actively control a pneumatically driven robotic device that can induce specific muscle force patterns in target muscles during a subject's voluntary movement. In this paper, the generation of constant forces in the rectus femoris muscle throughout the knee extension, i.e., isotonic contractions, was studied. Due to a highly nonlinear nature of mapping the joint torque to muscle force, a simple application of constant torques to the knee joint would not realize isotonic contractions. The proposed robotic exercise accounted for nonlinear moment arms of muscles as functions of joint angles and nonlinear coordination of multiple muscles in the neuromuscular system to accomplish individual muscle control. A pneumatically powered one degree of freedom (DOF) device that can impose active force feedback control has been designed and built. An exercise-planning algorithm has been developed that involved a musculoskeletal model of the lower-body, and the dynamics of a pneumatic actuator. Five constant force profiles were tested for twenty healthy volunteers and electromyographic (EMG) signals were collected while the device was applying calculated force profiles.

Keywords

Isolation exercise, muscle force control, isotonic contraction, muscle optimization, musculoskeletal model, lower extremities, pneumatically powered exercise device, electromyogram, rehabilitation

1. Introduction

With a rapid increase of median age, there is a need for healthcare technologies that enable an advanced physical exercise for maintaining or improving physical ability. Such a technology includes robotic exercise where an actively controlled robotic device applies programmed forces to realize a specific loading condition in a body part of interest. Certain situations in life bring a need to exercise a specific muscle, or a group of muscles, such as for fitness, rehabilitation, and neuromuscular function tests. Examples of such situations include isolated training of a leg muscle for maximum endurance. Muscle-isolation exercise could bring an extra degree of freedom to a physical therapist to have more control over what types of muscle forces they desire for their patients. This concept could also be used for athletic training purposes. Note that this paper does not aim to claim that isolated exercises are more efficient than compound exercises, or vice versa. Rather, the paper addresses technical difficulties in inducing a desired load in a target muscle in an “isolated” fashion.

The ultimate goal of this research is to establish a methodology to develop an actively controlled robotic device for inducing a specific muscle force pattern in a muscle of interest. To achieve this goal, the paper proposes robotic and computational methodologies to enable better-tailored isolated exercises than conventional methods. One might think that a certain torque profile applied to a joint would linearly appear in muscles involved in the movement around the joint. This is unfortunately not true in most of the muscle-force and joint-torque relationships in the human musculoskeletal system. This difficulty is primary due to two reasons: nonlinear moment arms of muscles as functions of joint angles and nonlinear coordination of multiple muscles in the neuromuscular system. Therefore, determining a joint torque profile that induces a desired muscle force profile in a target muscle is not straightforward.

Extensive research has been created over the years in regards to both assistive and resistive robotic machines such as the BLEEX exoskeleton²³, HAL-5 exoskeleton²⁴, active ankle-foot orthoses²⁵, active rehabilitation devices^{26,37}, resistive haptics using electrorheological fluids²⁷, fluid-powered exercise machines²⁸, etc. Contributions towards exoskeletons/robotic machines include modeling of human anatomy^{2,3}, modeling of various actuation technologies such as pneumatics²⁹, and different control techniques for these systems⁴. Such research on human-robot physical interaction ranges from mechanical design, sensing, and motion control of a device, to gait training and neuromuscular functional recovery. However, few research investigations have been conducted into selectively controlling individual muscle forces via human-robot interaction. This robot-assisted individual muscle control is a comprehensive concept. Neuromuscular function test, therapeutic training, force assisting, and isolation muscle training, can be boiled down to a single question: *How can we determine an adequate exercise that induces a desired change in a target muscle force?* With the current state of the art, procedures rely heavily on therapists’ knowledge or a too simplified assumption about the muscular system. Due to the highly nonlinear nature of mapping the joint torque to muscle force, the simplistic approach would be insufficient for accurately

controlling muscles^{20,30,31,32}. While studies on isotonic contractions in a specific muscle were reported in the literature^{33,34}, the mechanism of inducing isotonic contractions was not discussed. Planning an exercise for inducing a constant force during a change in muscle length is not straightforward in most of the muscles. Although individual muscle control is relatively complex, this is still a technically solvable problem by mathematically modeling the interaction between the robot and human musculoskeletal dynamics. Research for the upper body was first investigated by Ueda et al.^{1,35}. Outside of this research, however, a method for individually controlling muscles has never been studied in this particular way.

Individual muscle control is to induce specific muscle force profiles in target muscles during the subject's voluntary movement¹. This concept was first applied to the upper extremities using an exoskeleton-type wearable robot. The paper¹ showed some promising results and the proposed method could achieve desired changes in target muscles. However, this method had three key limitations. First, the previous algorithm could not directly specify desired magnitudes of muscle forces. It required a nominal task that provides a baseline of muscle activities. Muscle control was merely performed from the baseline by specifying ratios of change in target muscles. Second, tasks were limited to isometric tasks. Changes of muscle moment arms were not considered. Third, the muscle control algorithm was previously implemented in an off-line fashion. This paper describes a new approach that can resolve these issues so that the individual muscle control can be applied to non-isometric tasks in real-time.

An iterative numerical calculation method is proposed that is designed to allow for individual control of mono-articular or bi-articular muscles while not inhibiting the subject's range of motion. To apply the individual muscle control concept to non-isometric cases, the algorithm controls the device in an online fashion based on the changes of joint angles. Pre-calculated results are approximated by 4th order polynomials and stored in a controller. The lookup table approach enabled real-time muscle control.

This paper takes the knee extension exercise as a representative example and attempt to control the activity of the rectus femoris muscle, a bi-articular muscle that spans from the hip to knee joints. The rectus femoris muscle was chosen as the target muscle because such a superficial muscle is easily accessible using surface electromyograph (EMG) electrodes and the muscle is relatively large so that we could minimize the influence of crosstalk in surface EMG measurements. A pneumatically powered one degree of freedom (DOF) device has been designed and built. The device consists of a pneumatic cylinder actuator, position sensor, pressure sensors, pneumatic valves, and a real-time controller. The device is designed to resist the motion of the human knee by applying actuator forces in opposition to a specified muscle force profile. A custom-designed algorithm predicts and adjusts the wearer's muscle activities by using a musculoskeletal model of the leg. The device uses quasi-dynamic (useful for slow to moderate human movement speed) force-feedback control based on pressure measurements that determines the pneumatic actuator forces at desired positions and times. To make the evaluation simple, experiments aim at the generation of constant force in the rectus femoris muscle throughout the knee extension, i.e., realizing isotonic contractions in the

target muscle. According to the aforementioned reasons, application of constant knee joint torque during the knee extension would not realize constant muscle force.

A total of 20 healthy male and female volunteers with ages ranging from 20 to 35 participated in the experiments. Five constant muscle force profiles were tested as desired muscle force patterns. Surface EMG signals were recorded during the proposed exercises. For comparison, EMG signals while the device was applying constant knee torque were also recorded. Means and root-mean-square deviations of the recorded muscle forces were evaluated. It was confirmed that the proposed method was able to induce desired mean force levels with a statistical significance of $p < 0.05$. Results also showed that the proposed method realized (concentric) isotonic contractions with a 41 % smaller root-mean-square deviation in the EMG signal for a desired force of 200 N and with a 13% smaller root-mean-square deviation for a 550N force than simple application of constant knee torques.

2. Modeling and Control of Pneumatic Leg Exercising Device

2.1. Musculoskeletal Model of the Human Leg

A mathematical model of the human leg is necessary to represent the forces/torques induced onto the lower extremity by the interaction with a robotic device. **Figure 1** shows a 3-DOF (i.e., from the hip to the ankle joint) musculoskeletal model with nine major muscles of a human's lower limb². The muscles are shown in TABLE I numbered by using i ($i=1, 2 \dots 9$) with their maximal voluntary forces. The physical parameters of the human leg were taken from^{2,3} and are found in TABLE II.

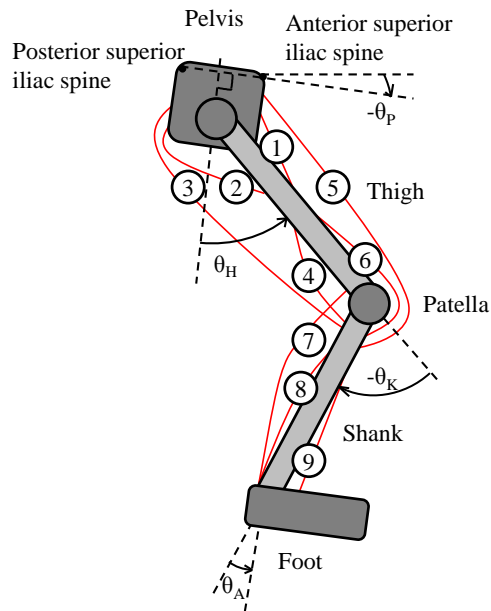


Figure 1: Musculoskeletal model of human lower extremity; Hip angle defined as angle between long axis of thigh and perpendicular line connecting the anterior superior iliac spine and posterior superior iliac spine

TABLE I
SPECIFIC MUSCLES AND MAXIMUM ISOMETRIC MUSCLE FORCE²

Muscle <i>i</i>	MUSCLE NAME	f_{MAX_i} (N)
1	Illiopsoas	1850
2	Gluteus Maximus/Medius	2370
3	Hamstrings	2190
4	Bicep Femoris (Short Head)	400
5	Rectus Femoris	1000
6	Vastus Intermedius	5200
7	Gastocnemius (Lat and Med. Head)	1600
8	Soleus (Plantarflexion)	3600
9	Tibialis Anterior (Dorsaflexion)	1100

TABLE II
ANTHROPOMETRIC DATA OF SHANK, THIGH, AND ANKLE

	Length (m)	Distance from proximal end to center of mass (m)
Thigh	0.5	0.244
Shank	0.45	0.279
Foot	N/A	*0.08

* Indicates hypotenuse length due to the center of mass being off-center of the shank axis

Angles θ_H , θ_K , and θ_A are the hip, knee, and ankle joint angles respectively. When these muscles defined in the musculoskeletal model shown in **Figure 1** are multiplied by their respective moment arms, the total muscle torques created at each joint can be obtained by

$$\boldsymbol{\tau}_{MUSCLE} = \mathbf{A}(\boldsymbol{\theta})^{3 \times 9} \mathbf{f}^{9 \times 1} \quad (1)$$

where $\boldsymbol{\tau}_{MUSCLE} = [M_H \quad M_K \quad M_A]^T$ are the torques applied by the skeletal muscles, and $\mathbf{A}(\boldsymbol{\theta})^{3 \times 9}$ is the moment arm matrix with moment arms of the 9 muscles with respect to the hip, knee, and ankle joint axes. The subscripts H , K , and A denote hip, knee, and ankle, respectively. $\boldsymbol{\theta} = [\theta_H \quad \theta_K \quad \theta_A]^T$ is the joint angle vector. $\mathbf{f}^{9 \times 1}$ is the force vector of the 9 muscles. Matrix $\mathbf{A}(\boldsymbol{\theta})^{3 \times 9}$ was created by a combination of several different studies on the hip, knee, and ankle joints, and the muscles and moment arms involved with each of these joints shown in TABLE III where $j = \{H \text{ (hip), } K \text{ (knee), } A \text{ (Ankle)}\}$. These equations are modified versions of the ones used in ².

TABLE III
MOMENT ARMS $A_{j \times n}$ OF MUSCLE GROUPS $n = 1 \dots 9$ (IN METERS, θ IN RADIANS; VALUES NOT SPECIFIED ARE EQUAL TO ZERO)

JOINT:	EQUATION:
Hip Joint:	$A_{H1} = 0.00233\theta_H^2 - 0.00223\theta_H - 0.0275$ $A_{H2} = -0.0098\theta_H^2 - 0.0054\theta_H + 0.0413$ $A_{H3} = -0.020\theta_H^2 - 0.024\theta_H + 0.055$ $A_{H5} = 0.025\theta_H^2 + 0.041\theta_H + 0.040$
Knee Joint:	$A_{K3} = -0.0098\theta_K^2 - 0.021\theta_K + 0.028$ $A_{K4} = -0.008\theta_K^2 - 0.027\theta_K + 0.014$ $A_{K5} = -0.058\exp(-2.0\theta_K^2)\sin(-\theta_K) - 0.0284$ $A_{K6} = -0.070\exp(-2.0\theta_K^2)\sin(-\theta_K) - 0.0250$ $A_{K7} = 0.018$
Ankle Joint:	$A_{A7} = 0.053$ $A_{A8} = 0.035$ $A_{A9} = 0.013(\theta_A + .637^\dagger) - 0.035$
\dagger : Ankle position offset defined in ²	

2.2. Robotic Exercise Device

A robotic device shown in **Figure 2** has been developed. The device consists of a Bimba pneumatic cylinder (097-DP), a force sensor (Omega LCM 703-50), Polhemus Fastrak motion tracker for position sensing, Festo proportional pneumatics valves (MPYE 05-M5-010-B), and Wika pressure sensors (Model A-10). Among other possible actuators, pneumatic actuation was chosen because of its safety, light weightness, and cost advantages¹. The pneumatic cylinder has a bore diameter of 26 mm, a stroke length of 18 cm, and the maximum force of approximately 800N at 1720 kPa supply pressure. In this device, the maximum force is approximately 400N with a compressed air supply up to 600 kPa. The friction of the pneumatic cylinder has been identified to be a combination of static friction of approximately 8.5 N and viscous friction whose coefficient was 35 Ns/m. The friction is partially compensated by adding an offset to the input command, which will be discussed in the next subsection. To minimize a possible influence of metallic materials in magnetic position measurements, the Polhemus sensors were mounted on plastic housings to avoid direct contact with the surface of the cylinder. The force sensor is used only to measure the force that the pneumatic cylinder applied to the leg for evaluation and is not used for feedback control purposes. Instead, the pressure sensors are used to control the actuator force in a semi-closed loop fashion. A National Instruments data acquisition board (NI-USB-6229) connected to a computer running LabVIEW is used for data collection at a sample rate of 200Hz. A surface EMG measurement device by Run Technologies (Myopac Jr., analog output frequency of 8kHz) recorded real-time EMG signals coming from the muscle for assessment.

An experiment specific diagram is shown in **Figure 3** where one pneumatic actuator connects the wall and shank, applying torque against the knee joint. Let $\boldsymbol{\tau}_{ACTUATOR} = [\tau_H \quad \tau_K \quad \tau_A]^T$ be the torque vector with torques produced by the robotic device given by

$$\boldsymbol{\tau}_{ACTUATOR} = \mathbf{B}(\boldsymbol{\theta})^{3 \times 3} \mathbf{F}^{3 \times 1} \quad (2)$$

where $\mathbf{B}(\boldsymbol{\theta})^{3 \times 3}$ is a moment arm matrix of the pneumatic device as a function of the posture of the leg. The components of $\mathbf{B}(\boldsymbol{\theta})^{3 \times 3}$ can easily be obtained from the kinematics of the robotic device³⁶. $\mathbf{F}^{3 \times 1} = [F_H \quad F_K \quad F_A]^T$ is the general force vector for the forces produced by the pneumatic actuator that counteracts muscle forces produced at the hip, knee, and ankle joints. With a single pneumatic actuator as shown in **Figure 3**, the force vector is defined as $\mathbf{F}^{3 \times 1} = [0 \quad F_K \quad 0]^T$.

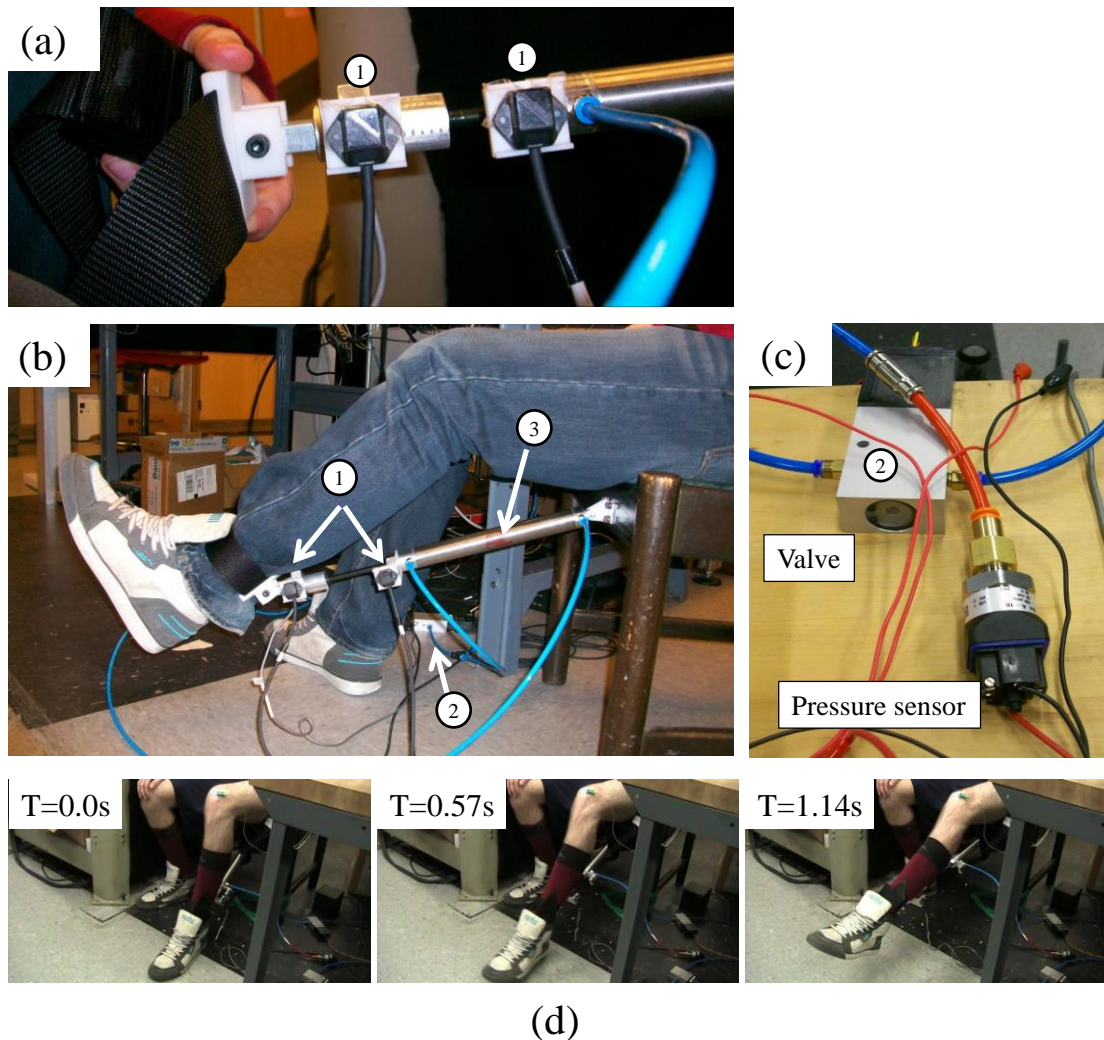


Figure 2: Physical Prototype: (a) Position sensors (1) and Pneumatic cylinder (3); (b) Device overview; (c) Pneumatic valve (2) and pressure sensor; (d) Knee extension exercise at around 0.5Hz.

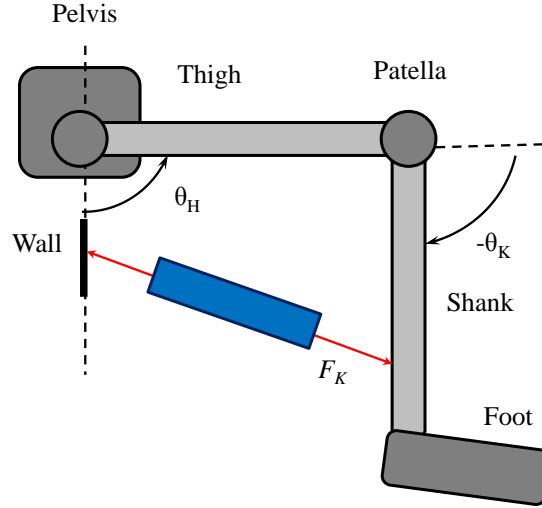


Figure 3: Kinematic model with a pneumatic actuator attached to a chair in the experimental setup. The Pelvis is assumed to be fixed in place as a wall.

Although a fully dynamic model of the leg can be derived from³, this paper uses a quasi-dynamic model by neglecting the inertia, centrifugal, and Coriolis terms, i.e.,

$$\tau_{MUSCLE} + \mathbf{g}(\boldsymbol{\theta}) + \tau_{ACTUATOR} = 0 \quad (3)$$

where $\mathbf{g}(\boldsymbol{\theta})$ is a gravity torque vector. Note that the dropped terms contribute less than 3% of the total joint torques needed for the knee movements tested in this paper where the dynamics of the pneumatic system are more dominant and the user is performing the exercise in a slow and controlled manner³⁶. Therefore, we judged that the quasi-dynamic model of the leg would be sufficient in this paper.

2.3. Pneumatic System Modeling

2.3.1. Force Generation by Pneumatic Cylinder

In this research, pneumatic actuation was chosen to generate resistive forces against the muscle forces to induce a specific muscle force profile in the rectus femoris muscle. A typical pneumatic actuator can be modeled as shown in **Figure 4**. The work by Shen *et al.*⁴ shows how using two 3-way proportional valves rather than one 4-way valve can be used to independently control the force and stiffness of a pneumatic actuator. This paper uses a similar approach to accomplish force control by controlling pressures in two chambers.

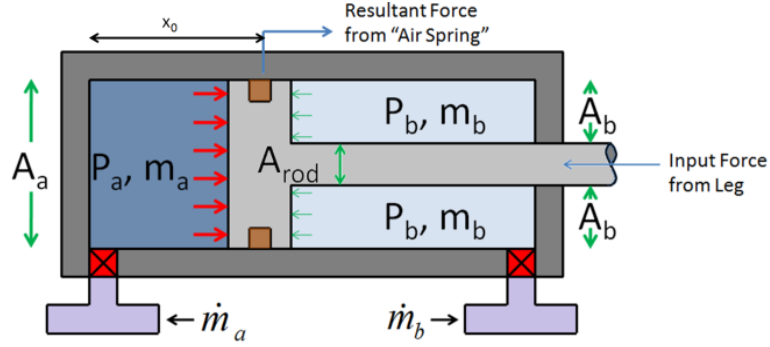


Figure 4: Schematic of pneumatic actuator

In **Figure 4**, P_a and P_b are pressures inside each chamber of a pneumatic cylinder actuator where m_a , m_b , and \dot{m}_a , \dot{m}_b , are the masses of air and change of masses on each side of the piston. A_a and A_b are the effective areas of each side of the piston, and A_{rod} is the cross-sectional area of the piston rod. The force generated by the pneumatic actuator is given by

$$F_K = P_a A_a - P_b A_b - P_{atm} A_{rod} \quad (4)$$

$$F_{Actual} = F_K + F_{Friction} \quad (5)$$

where P_{atm} is the atmospheric pressure and $F_{Friction}$ is the resistive force of friction against movement. F_{Actual} is the actual force that is applied to the leg including friction forces. Unlike the previous research that aimed at position control^{4,5,7,45}, the research focuses on controlling force, F_K , and the position of the actuator is passively determined by the interaction with the human. As can be found in (4), measurement and control of P_a and P_b would achieve force control.

2.3.2. Semi-Closed Loop Force Control of the Pneumatic Actuator based on Pressure Sensing

The experiments were conducted at relatively low frequencies. The dynamics of the servovalve spool, from current input of the proportional value to the area of the spool value A_{SPOOL} , can be either neglected^{4,45} or approximated as a linear phase-lag transfer function⁵ since the valve dynamics is significantly faster than that of the chamber dynamics in the pneumatic actuator. As reported in the literature^{4,5,7,45}, the dynamics of chamber pressure, e.g., P_a , is nonlinear and can be represented by \dot{m}_a , the ratio between upstream and downstream pressure, and other factors. To compensate for the nonlinearity of the pneumatic system and achieve force control, force-feedback control based on pressure measurements as shown in **Figure 5** was implemented.

In **Figure 5** a force controller using Proportional-Integral (PI) pressure feedback in the form of $K_p + \frac{K_I}{s}$ in the Laplace domain was used. Instead of a full closed-loop using a force sensor, this architecture forms a semi-closed loop using pressure measurements from which the force was estimated by using (4) for improved response of the closed-

loop system. The gains $K_P = 0.065$ and $K_I = 0.02$ were determined by trial-and-error to yield a resultant force that matched as close as possible to the reference force signal.

2.3.3. Compensation of Friction

Both static friction (stiction) and dynamic (viscous) friction are addressed for frictions in (5). The static friction is a function of the seals and lubrication used within the pneumatic cylinder assembly and is normally considered as a fixed value. Viscous friction is a function of the speed at which the system moves and is normally based upon interactions of cylinder components as well as the potential of compressibility of the air within the cylinder itself. There are various methods for modeling the friction^{6,7,8}. In this paper, a small dither signal was added to the position reference signal to keep the system constantly vibrating minutely to focus only on the viscous friction component and not the stiction component. The viscous friction component has been modeled using an empirical approach and added to the overall control method as a feed-forward input.

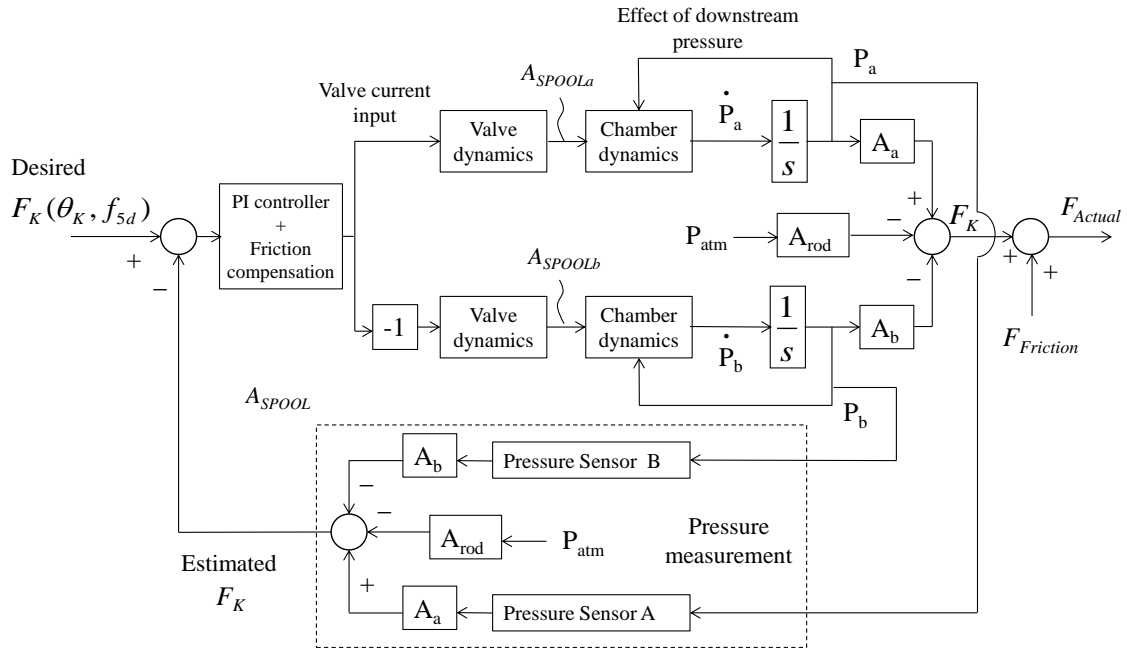


Figure 5: Semi-closed loop PI pressure feedback for force control

2.4. Experimental Validation Pressure-based Force Control

To show that the proposed method of force control is a viable option, validation experiments have been conducted through tracking a sinusoidal force at varying frequencies. This research requires the device to be able to respond to a normal human's exercise frequency under load. This movement was found to be < 0.5 Hz for the range of motion of the knee. This 0.5 Hz frequency was found through experimentation of the authors for testing out a moderate load on the leg and moving it through its range of motion from a 90 degree knee bend to around 45 degree knee bend. **Figure 6** shows the results of the semi-closed loop control experiments to determine how well the force

(pressure derived) feedback control could track a sinusoidal force signal oscillating between 20% and 80% of the supply pressure at various frequencies.

As shown in the figure, the proposed semi-closed loop system can reasonably track a sinusoidal force at least at a frequency of 1 Hz using the pressure sensors when compared against the actual force measured by using the force sensor. For frequencies higher than 1 Hz, there seems to be more phase lag and less of an ability to track the force reference signal under the current setup. After 1 Hz, it was found that the force sensor and the pressure sensors would begin to display different forces indicating that pressure-sensor semi-closed loop control works for force control accurately up to 1 Hz. Consequently, this force control method sufficiently performs for the leg exercise considered in this paper. To achieve a more accurate performance in force control at faster speeds, different modeling approaches would be necessary. This limitation for future application will be addressed in the discussion section.

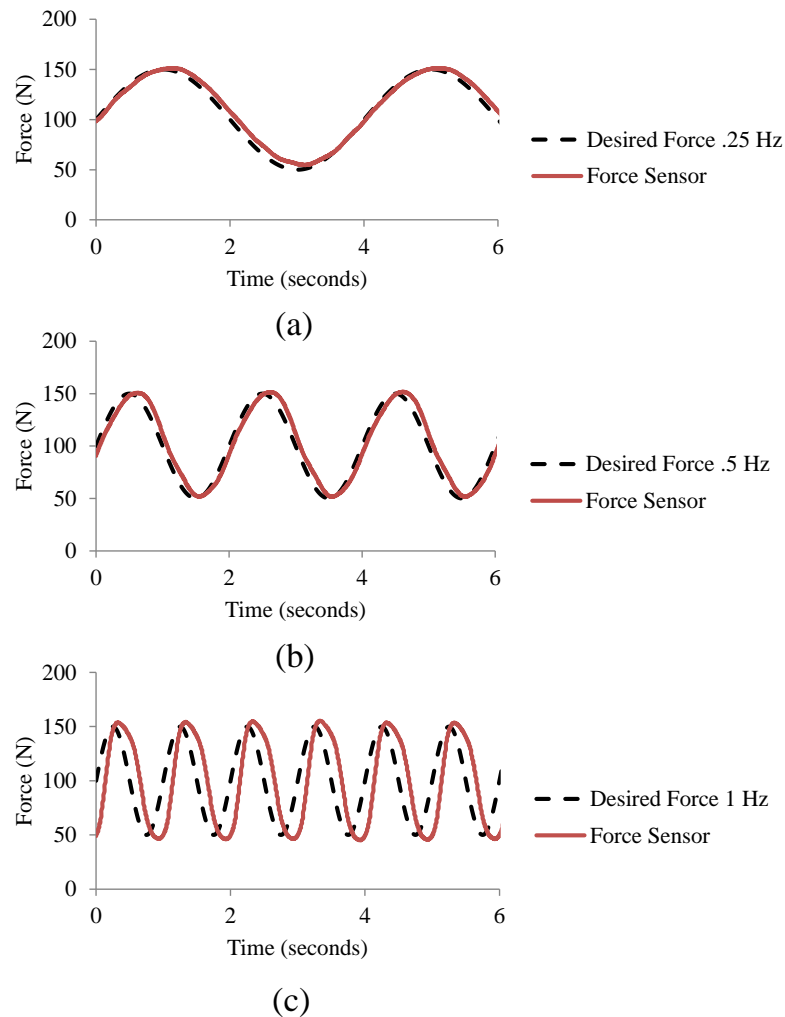


Figure 6: Semi-Closed Loop force feedback following a sinusoidal reference force oscillating between 20% and 80% of supply pressure. The figures range in frequency of .25 Hz to 1 Hz. (a) 0.25 Hz; (b) 0.5 Hz; (c) 1.0 Hz

3. Muscle Force Control

3.1. Optimization Method to Predict Muscle Forces

This section briefly explains an existing muscle-force prediction technique based on the optimization principle in the neuromuscular system⁹. Note that this type of muscle force prediction is a well-known, established technique. The force prediction method will be implemented as a part of the proposed algorithm to inversely *control* muscle forces explained in the following section.

From (1), if $\boldsymbol{\tau}_{MUSCLE}$ and $\mathbf{A}(\boldsymbol{\theta})$ are given, the force vector, \mathbf{f} can be calculated through a static optimization method utilizing a cost function proposed in the literature⁹. A physiology-based cost function hypothesizes that the nervous system seeks to minimize the overall effort in regards to which muscles should activate to realize the given joint torques. This cost function is expressed as

$$\begin{aligned} \text{Minimize} \quad & u(\mathbf{f}) = \sum_{i=1}^n (c_i f_i)^r & (6) \\ \text{Subject to} \quad & \begin{cases} \boldsymbol{\tau}_{MUSCLE} = \mathbf{A}(\boldsymbol{\theta})\mathbf{f} \\ 0 \leq f_i \leq f_{MAX_i} \quad (i = 1, \dots, n) \end{cases} \end{aligned}$$

where $u(\mathbf{f})$ is a cost function, c_i 's are the weighting factors, r is an integer number, f_i is force of the i -th muscle, and f_{MAX_i} is the maximum muscle force of the i -th muscle. The maximum muscle forces are given according to³ as shown in TABLE I. The cost function determines a minimized solution for the muscle forces subject to given constraints. For the cost function, the weighting factors c_i 's will be defined as

$$c_i = \frac{1}{PCSA_i} \quad (7)$$

where $PCSA_i$ is the physiological cross sectional area of the muscle (PCSA), and $PCSA_i = f_{MAX_i} / \sigma_{MUSCLE}$, where $\sigma_{MUSCLE} = 31.39 \text{ N/cm}^2$ was used according to¹⁰. In this paper, the value of $r = 2$ is used as one of the recommended choices⁹. It should be noted that there are studies using other possible values and choices of weighting factors^{9,11,12}. The computation is easily implemented by using the `quadprog` or `fmincon` functions in MATLAB. In this paper, the `quadprog` function was used.

There are arguments and criticisms however regarding the neurological background and limitations of this prediction. One argument in particular for this method could be that there is a potential limitation of a minimization function because it cannot take into account co-contraction of the muscles for increasing stiffness. However, the effectiveness of this method for predicting stereotypical muscle performance has been reported in a number of papers such as^{13,14,15,16}. There are additional proposed methods such as muscle synergy and various other methods^{17,18,19}. Some muscle force prediction software

packages are commercially available^{38,39}. Furthermore, recent studies show that muscle activation in persons with crouch gait can be predicted if the musculoskeletal model is modified appropriately⁴⁰.

3.2. Desired Activation Profiles of the Rectus Femoris Muscle

Attention is focused on a muscle control method with a desired muscle profile for the rectus femoris muscle, one of the nine lower-extremity muscles modeled in **Figure 1**. To make the evaluation and discussion simple, this research attempts to generate constant force profiles throughout the knee extension regardless of the knee angle. In other words, the robotic device is controlled such that isotonic contractions are realized in the rectus femoris muscle, i.e., f_5 . The experiment tested five different constant muscle force levels, at 87.5N increments between each muscle set throughout the range of motion of the knee as shown in TABLE IV. The range of forces, from 20% to 55% of the maximum voluntary force of the rectus femoris muscle, has been chosen based upon the hardware limitations of the system for the maximum force. The experiment involves subjecting healthy volunteers to these five different muscle force profiles and recording the surface EMG signals that result from the forces imposed on the leg due to gravity and the actuator.

TABLE IV
Desired Isotonic Muscle Force Profile Sets

SET	DESIRED MUSCLE FORCE PROFILE FOR f_{5d} (N)
1	200
2	287.5
3	375
4	462.5
5	550

Conventional wisdom may suggest that constant joint torque (or force) application would be sufficient to induce a constant muscle force throughout knee extension. Unfortunately, such a simple application of constant knee torques would not realize isotonic contractions since a) the moment arm of the muscle changes as the knee angle changes as shown in TABLE III, and b) there are multiple muscles involved in the exercise, therefore the distribution among the contributing muscles is determined by the optimization shown in (8).

Regarding the issue a), an example of the rectus femoris moment arm to the knee joint is shown in **Figure 7**. The moment arm was calculated based on TABLE III, varying the knee angle θ_K and fixing the hip angle. **Figure 7** indicates that a constant muscle force would not generate a constant knee torque. Conversely, an exercise that applies a constant knee torque never induces a constant muscle force in the rectus femoris muscle. The aforementioned issue b), coordination of multiple muscles in the neuromuscular system, must be resolved. If only one muscle is responsible for a particular joint motion, one could inversely solve for the actuator torques that would induce muscle forces within a desired muscle profile by considering the change of the moment arm. However, as

reported in ²⁰, except for the first dorsal interosseus (FDI) muscle for the abduction of the index finger metacarpophalangeal joint, such a simple muscle-joint relationship is rare in the human musculoskeletal system. Even in the simplified model shown in **Figure 1**, the rectus femoris muscle couples with the vastus intermedius muscle for the knee extension.

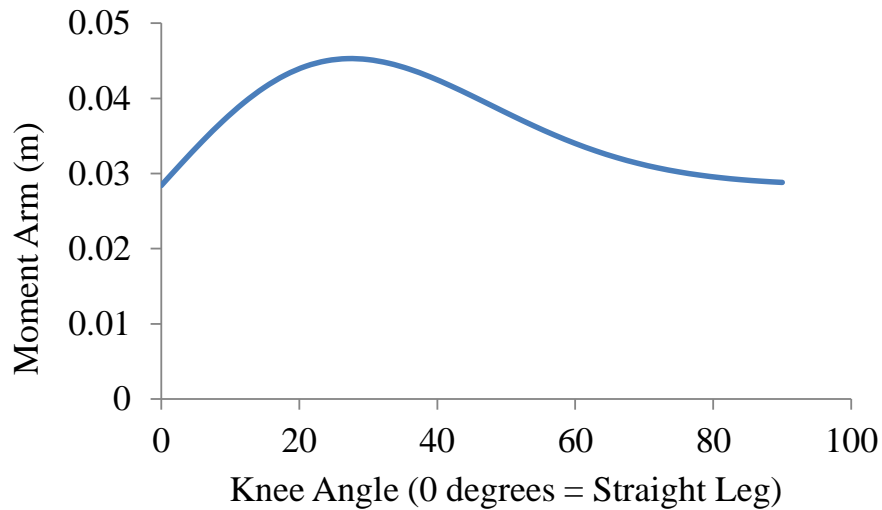


Figure 7: Moment arm of the rectus femoris muscle by varying the knee angle and fixing the hip angle

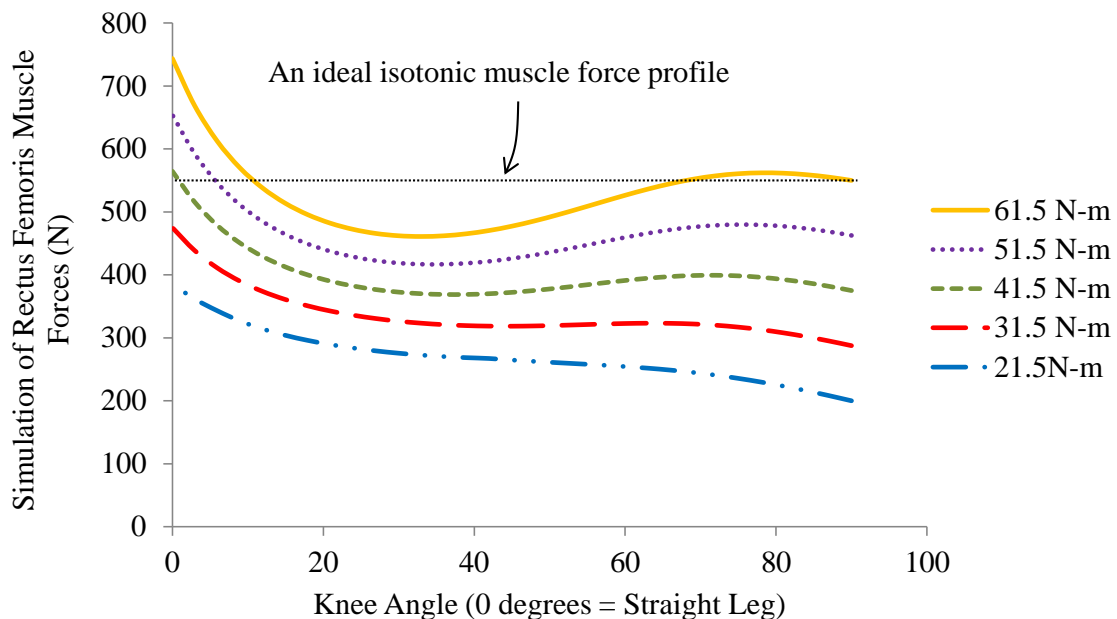


Figure 8: Simulation results of five constant knee joint torques and corresponding muscle forces: Due to the nonlinearities in muscle force generation, constant joint torques were not able to induce constant muscle forces.

To illustrate the difficulty of individual muscle control, numerical analysis was conducted by implementing the muscle prediction method explained in the previous section. **Figure 8** shows the simulation results of the activity of the rectus femoris muscle when applying five different constant torques against the knee joint. As expected, constant knee torques did not necessarily induce constant forces, or isotonic contractions, and exhibited deviations from a constant force. This observation will be confirmed by experiments in a later section. As a result, a method besides constant joint torque application is necessary if an experimental protocol wants to be able to induce a constant force in a target muscle.

3.3. Obtaining Actuator Forces to Realize Desired Force Profiles in a Target Muscle

The process of finding the pneumatic actuator forces to create a desired muscle force has also been investigated by one of the authors¹. However, the previous algorithm could not directly specify desired magnitudes of muscle forces. Instead, muscle control was performed by specifying ratios of change in target muscles from a baseline of muscle activities obtained for a nominal task. In addition, only isometric tasks were considered. Furthermore, the former algorithm to determine robot actuator forces was completely off-line, not capable of adjusting forces to a change of the posture during experiments. To overcome these limitations, a new algorithm has been developed in this paper that consists of two parts: a MATLAB based offline program for interactively calculating actuator forces and a LabVIEW based online program for controlling the robotic device with pressure-derived force feedback.

A flow chart of the proposed iterative method is shown in **Figure 9**. A desired muscle force is the input to the algorithm. In this particular study, a desired force for the rectus femoris muscle, or f_{5d} , is specified. To realize isotonic contractions, constant forces shown in TABLE IV are used. Note that this algorithm can also accept any desired force as a function of the joint angle. The program uses the musculoskeletal model discussed in 2.1 to determine what torque, τ_K , is needed to impose from the actuator to the knee joint. The program then uses the minimization function to predict what the muscle force would be induced in the target muscle at a given joint angle. If the predicted force, \hat{f}_5 , is not within the threshold, the system changes the actuator torque and runs the iterative method again until the predicted force falls within the threshold ε . In this paper, $\varepsilon = 0.01$ was chosen by trial and error. If the output force is within the threshold of being close to the desired muscle force, the pneumatic actuator force is calculated based on (2) and the result is stored in a database as a function of the desired force and joint angle, i.e.,

$$F_K(\theta_K, f_{5d}).$$

The program then increments the joint angle and continues the calculations until it covers a given range of joint motion. Resultant actuator force profiles are shown in **Figure 10** for the rectus femoris muscle as the knee extends for the desired force sets in TABLE IV. In **Figure 10**, the actuator force is mostly negative, pulling the leg and resisting the knee extension. For the smallest values of desired muscle force (200N and 287.5N), at close to 0 degrees (straight leg), the gravity term imposes greater muscle force than the desired

force. Only in this situation, the actuator produces positive forces, i.e., pushing the leg up and assisting the knee extension. Results show that the actuator must produce a non-constant actuator force as a function of the knee angle to induce a constant muscle force, i.e., isotonic contraction, in the target muscle.

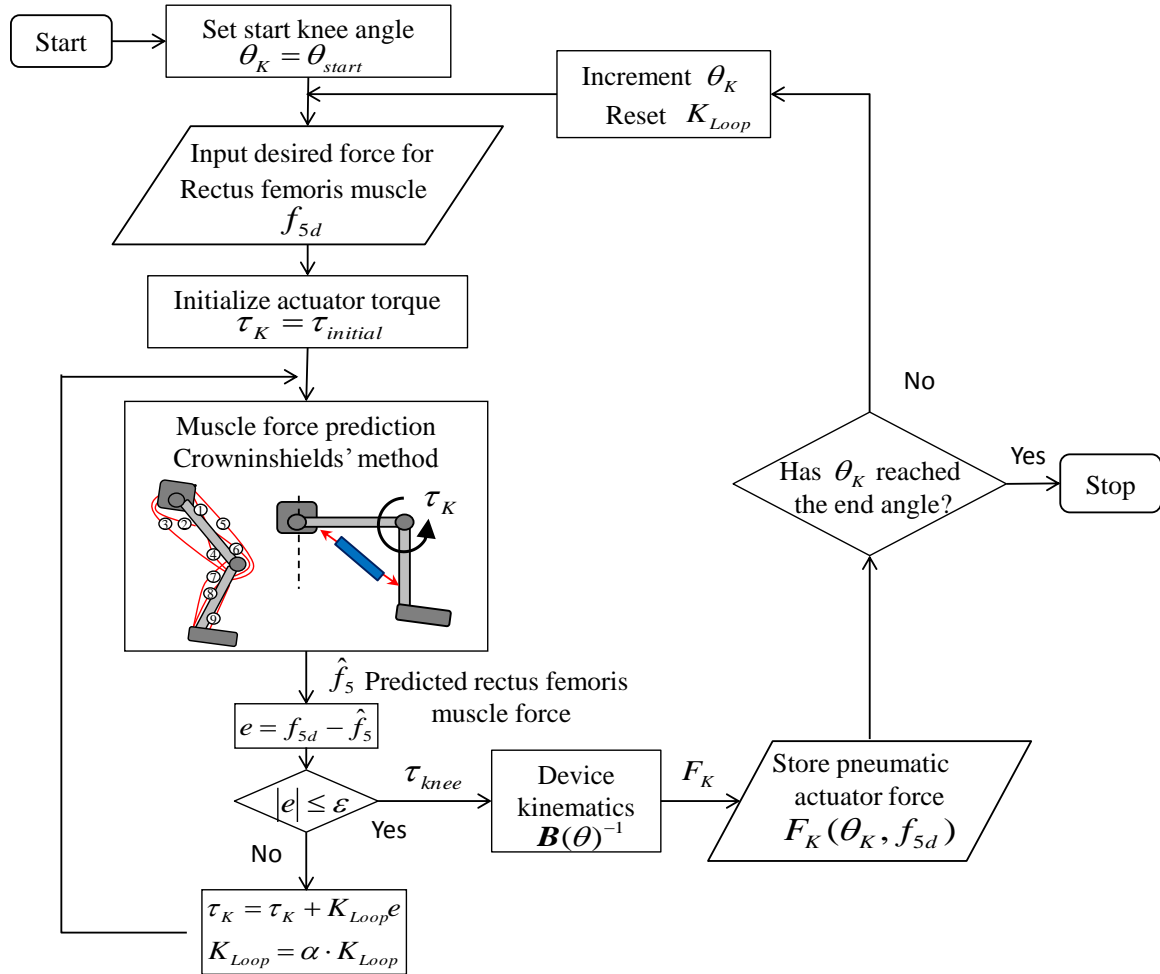


Figure 9: Flow chart of the iterative method for actuator force calculation

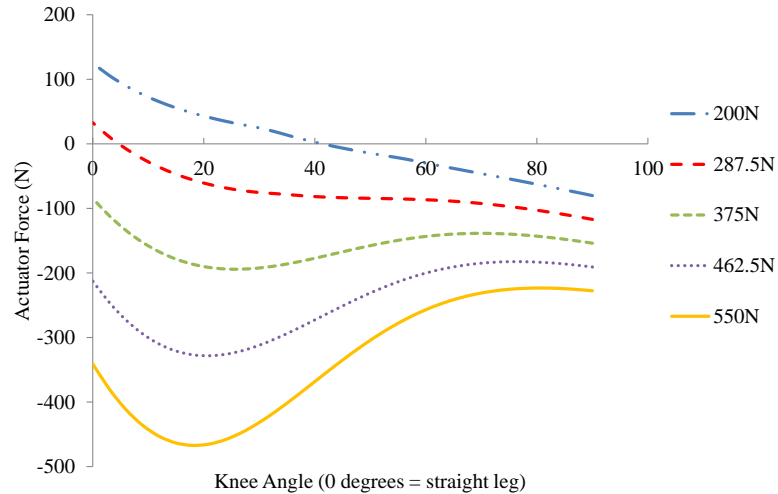


Figure 10: Actuator force profiles to realize desired constant forces in the rectus femoris muscle

3.4. Implementation

The force feedback control based on pressure measurement explained in 2.4 has been implemented onto a LabVIEW-based system. Because the posture and speed changes every time step, the program must adapt for this. It is not a realistic option to run the aforementioned MATLAB interaction method at every sampling period. Instead, each of the stored force profile curves, shown in **Figure 10** is fitted to a fourth order polynomial as a function of the knee angle. The robotic device measures the angle of the knee joint as well as length and velocity of the pneumatic cylinder by using the Polhemus Fastrak motion tracker shown in **Figure 2**. The LabVIEW program then uses the polynomial function and chooses the actuator force based on the current knee angle. This helps to save a large amount of computational time by eliminating the inner MATLAB loop. The measured cylinder velocity was also used to compensate for frictions in the pneumatic cylinder.

4. Experiments

4.1. Subjects and Method

A total of 20 healthy male and female volunteers with ages ranging from 20 to 35 participated in the experiment. IRB protocol H12069 approved by the Georgia Institute of Technology Office of Research Integrity Assurance was followed. The subjects were asked to attach the force-feedback pneumatic cylinder device to do different weights/force-profiles of a knee extension exercise. The subjects were also asked to wear an EMG measurement device on their leg, which measured muscle activation in the rectus femoris muscle with small electrodes. Before the experiment, each subject spent some time practicing with the device to become accustomed to it. Subjects then performed 10 repetitions for each muscle profile set tested and then rested for a 2-3 minute interval to minimize the effect of fatigue. For all sets, EMG sensor readings were

recorded, as well as displacement and force information from the position sensors, pressure sensors and force sensor. The subjects were asked to try to maintain a constant, isokinetic slow velocity and to keep the hip and ankle angles constant. Each experiment was run 10 times moving from 90 degrees to 45 degrees (straight leg is represented by 0 degree) of the knee. Surface EMG signals were filtered by using a Butterworth low-pass filter with a cut-off frequency of 2Hz and rectified. EMG values were normalized to their maximum voluntary contraction of each subject.

This paper assumed that processed EMG signals could closely approximate corresponding muscle forces. It is suggested in the literature that EMG and force are not necessarily linear in isotonic conditions⁴¹. Although there is no consensus as to how to precisely interpret EMG signals in dynamic movements, EMG signals have been practically used in gait and other dynamic movement analysis⁴². Relationships that could influence the force produced by a muscle relative to its activation, e.g., force-velocity, force-length, and fatigue, reported in the literature, were not used in the signal processing to simplify the analysis. The knee velocity tested in the experimental section was low enough for the concentric muscle exercise ($< 45^\circ \text{ s}^{-1}$) that the EMG results were also negligibly affected by the knee velocity^{21,22}. Muscle fatigue and recovery are difficult to model. Therefore, in the protocol, the profile sets were tested in a randomized order. With the 2-3 minute rest interval, this paper judged that muscle fatigue was negligible in the analysis. The authors recognize there is still a lack of precision in the assessment. These limitations will be described in the Discussion section.

4.2. Comparison between the Proposed Method and Constant Knee Torque Application for Robotic Isotonic Exercise

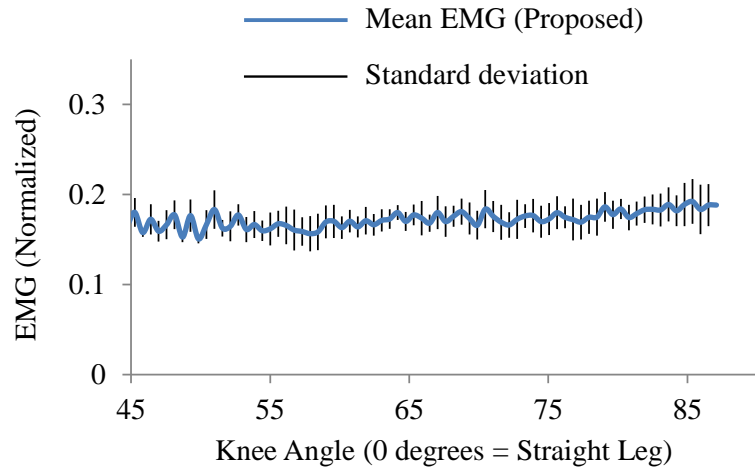
To illustrate the efficacy of the proposed method for realizing isotonic contractions, a comparison has been made between the proposed muscle control algorithm with the interactive method and simple application of knee torques that was discussed in 3.2. As shown in **Figure 8**, the application of a constant joint torque would not necessarily induce a constant force profile in the muscle that actually varies as the knee joint angle changes. Therefore, deviation of target muscle force from a constant muscle force profile should indicate how much a realized force profile is close to isotonic contraction. This index may be calculated by evaluating the root-mean-square deviations of rectified EMG signals throughout the range of the joint angle.

A benchmark was conducted by creating a constant torque profile corresponding to two of the muscle force profiles, $f_{5d}=200 \text{ N}$ and $f_{5d}=550 \text{ N}$, shown in TABLE IV. The joint torque at the initial joint angle was calculated by using the proposed method and the calculated actuator force was applied to the leg throughout the range of motion. To make a comparison between the proposed approach and constant joint torque application, with 21.5 N-m for $f_{5d}=200 \text{ N}$ and 61.5 N-m for $f_{5d}=550 \text{ N}$ respectively. **Figure 11** shows representative EMG measurements versus joint angle collected from one of the subjects. The plots show the average (mean) and standard deviation of 10 repetitions for $f_{5d}=200 \text{ N}$ grouped in 0.5 degree increments. For example, at the knee angle is 60 degrees, this average data point is the culmination of the data points from all of 10 repetitions between

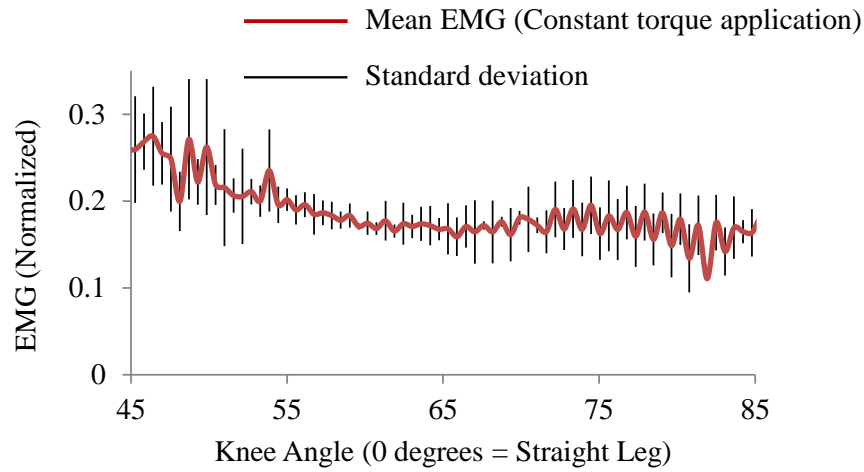
60 and 60.5 degrees. The standard deviations were then calculated for these data sets to create a standard deviation for each 0.5 degree increment. **Figure 11 (a)** shows the result of the proposed method and **Figure 11 (b)** shows the result of the constant torque application. The result shows that the proposed approach of controlling the target muscle force performs better than conventional approach of applying constant joint torque.

To perform a quantitative assessment between the proposed method and the constant torque application method for the same subject, root-mean-square deviations of induced EMG signals over the range of motion were calculated. A single datum point is generated from EMG measurement at every .5 degree increments of the leg movement, and the root-mean-square deviation was found by evaluated all these data points in the entire range of motion. In other words, this index shows the deviation from an average EMG in the range of motion, which is ideally expected to be constant. **Figure 12** shows the indices for $f_{5d} = 200$ N and 550 N compared with corresponding constant torque applications. The results were normalized by the result of constant torque application. The root-mean-square deviations shown in the figure were found to be lower by 41% using the proposed method for a 200N desired muscle force and lower by 13% for a 550N desired muscle force, than the application of constant torques, respectively.

While this benchmark test has been conducted for only one subject, **Figures 11 and 12** showed that the proposed muscle control method did reduce the deviation in the EMG data and resulted in a more constant muscle force overall. The results showed promise towards of the validity of the proposed method for arbitrarily controlling muscles forces through the musculoskeletal model and robotic device. The following experiment will further investigate this effectiveness for a larger population ($N=20$).



(a)



(b)

Figure 11: Comparison between the proposed method and constant torque application for isotonic exercise for muscle profile set 1 ($f_{5d}=200$ N) for one subject ($N=1$): Average EMG versus joint angle over 10 trials: (a) proposed method; (b) simple constant torque application of 21.5N -m.

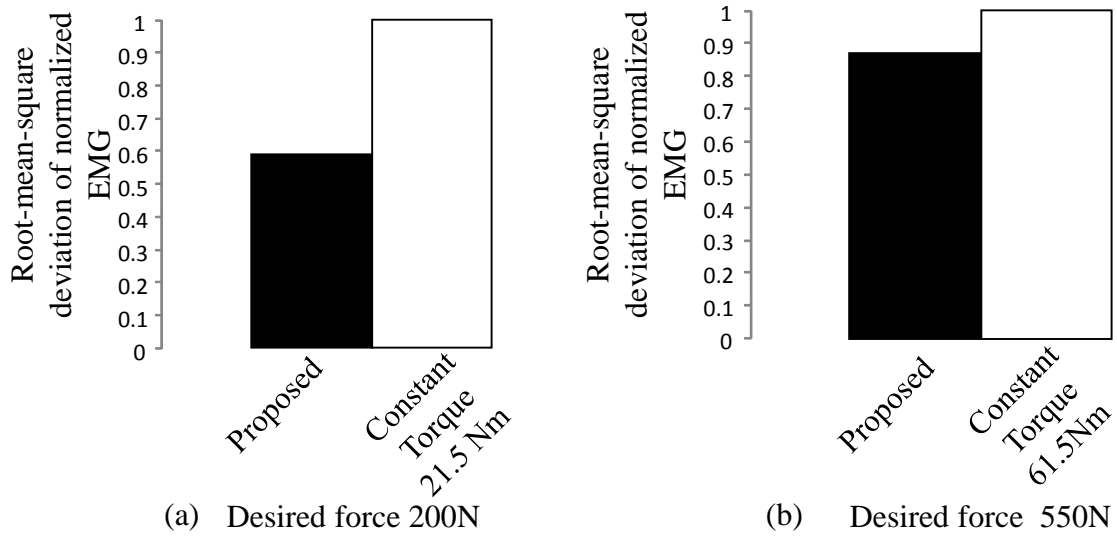


Figure 12: Comparison between the proposed method and constant torque application method for one subject ($N=1$). Root-mean-square deviations of the rectified EMG signals over the range of motion were evaluated: (a) muscle profile set 1 ($f_{5d}=200$ N) and corresponding constant torque application of 21.5 N-m; (b) muscle profile set 5 ($f_{5d}=550$ N) and corresponding constant torque application of 61.5 N-m.

4.3. Inducing Different Levels of Isotonic Contractions

It is expected that the proposed method can induce different levels of the rectus femoris muscle force as given in TABLE IV. To perform a quantitative assessment of the proposed method, the data was processed for twenty subjects ($N=20$) in the same manner as in Figure 12. Recall that the desired force levels given in TABLE IV were evenly spaced in a linear profile (87.5N increments). Results of the normalized EMG data of the proposed method that was conducted with the twenty healthy subjects are shown in **Figure 13**. Experimental mean values are well aligned on a straight line with $R^2=0.9934$, indicating that the proposed method is able to induce a desired force with a reasonable accuracy. A statistical significance with $p < 0.05$ using a one-tailed t-test was observed between Sets 1 and 2, 3 and 4, and 4 and 5, respectively. The confidence between Sets 2 and 3 was 93%. The benchmark test presented in 4.2 indicated that the constant knee torque application would introduce larger root-mean-square deviations in muscle activity. The statistical significance shown in **Figure 13** could not have been obtained if the proposed method had not been used.

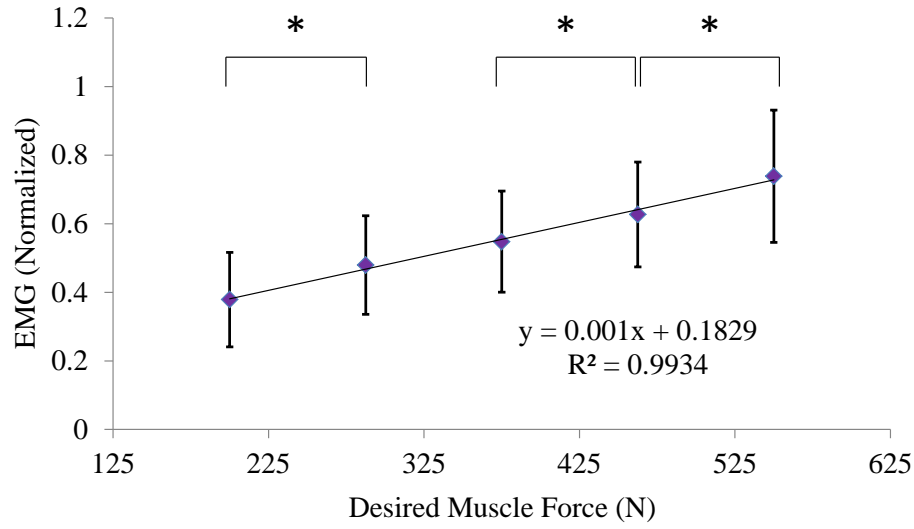


Figure 13: Muscle profile sets 1 through 5 and corresponding average normalized EMG values, the black lines indicate the root-mean-squared deviation of the data for twenty subjects ($N=20$); an “*” indicates a confidence of $p < 0.05$ when comparing the two sets to one another.

5. Discussion

Although this paper has presented promising results in terms of individual muscle control in dynamic movements, several issues remain unresolved and must be addressed in the future work.

Hardware and control limitation

The current control technique of an active quasi-dynamic force-feedback was able to track and realize a desired muscle force curve due to a human’s low to moderate speeds (< 0.5 Hz or $< .15$ m/s) during exercise. If the system is to be used for quicker movements (such as running), this particular system might not be able to create desired force quick enough for the user (i.e., hardware issue) or the actual force from pressure/force sensors would lag the desired force signal by too much (i.e., controls issue). The maximum force and speed of response could be increased by using a pneumatic cylinder with a larger bore size and a valve with a larger outlet. From a controls standpoint, more advanced control would be necessary to compensate for higher velocity through methods such as more accurate dynamics modeling or prediction-based control for repetitive motion.

Assessment of muscle forces via EMG signals

The lack of reliable methods to assess muscle forces using EMG in dynamic movements affects the quality of assessment. The evaluation presented in this paper assumed that processed EMG signals could closely approximate corresponding muscle forces. Such

analysis is a common practice in dynamic movement analysis such as gait and reaching due to the difficulties in incorporating relationships, such as force-velocity, force-length, and fatigue, into evaluation. These relationships are known to, sometimes significantly, influence the linearity assumption between muscle activation and produced force, which should be addressed in the future work. A possible alternative to EMG measurement is ultrasound elastography where muscle shear modulus is reported to be closely proportional to the magnitude of muscle force⁴⁴. In **Figure 12**, a larger deviation of EMG was observed at the higher desired force. One might recall signal-dependent force variability in isometric contractions reported in the literature. Due to limited study on force variability in non-isometric tasks, more research should be conducted for which the methodology developed in this paper may be used. This research is expected to provide a tool to adjust individual muscle forces in not only isometric tasks, but also isotonic tasks, enabling future neuromuscular research using ultrasound elastography and other techniques.

Co-contraction and other muscle force activities

The muscle force prediction method explained in 3.1 is known to be unable to predict possible co-contraction. Co-contraction is represented as the redundancy of muscle force prediction, represented as the null-space of the mapping of muscle forces to joint torques. This varies between subjects and trials possibly dependent on certain physiological or cognitive status. It was assumed that the subjects were well familiarized with the leg exercise performing practice tasks and could reproduce consistent movements. This assumption should be revisited and investigated. In addition, the proposed muscle control method focused on the control of the rectus femoris muscle and neglected the activities of other muscles. This limitation is because the device with one DOF was used for controlling a single muscle where there is no redundancy in controlling non-target muscles in this paper. Note that the generalized individual muscle control technique¹ can minimize the changes in non-target muscles by using a multiple DOF device such as an exoskeleton worn by the user that we plan to develop in the future.

Adjusting the musculoskeletal model

Strictly speaking, physiological parameters of muscles such as lengths, areas, maximum forces, and moment arms, are different between individuals; therefore those differences should be incorporated into the musculoskeletal model. For example, $A(\theta)$ matrix may need to be adjusted for more accurate muscle control. This paper used a single musculoskeletal model without such adjustment as we judged that variations associated with muscle force fluctuation and EMG data (i.e., noise) would be much larger than prediction errors associated with inaccuracy of physiological parameters. Individual differences may be incorporated in the figure by using an existing database (e.g. ⁴³ for the upper extremity). Further assessment of the proposed method within a larger population must be conducted.

6. Conclusions

By taking isotonic exercises of the rectus femoris muscle, this paper demonstrated that it was possible to induce a desired force in the target muscle with a lower root-mean-square deviation than the conventional approach. The results also demonstrated the usefulness of

the proposed iterative calculation of robot actuator forces, implementation into a real-time system, and pressure-based force feedback control of a pneumatic robotic device.

Five different constant muscle forces, sets 1 to 5 in the increasing order of the desired force, were tested for 20 healthy volunteers. Results show that mean values of normalized EMG data were well aligned on a straight line with $R^2=0.9934$, indicating that the proposed method was able to induce a desired activation level with a reasonable accuracy. A statistical significance with $p < 0.05$ was observed between Sets 1 and 2, 3 and 4, and 4 and 5, respectively. The proposed method obtained results with a high degree of confidence in induced forces for desired forces at 87.5N increments. Another comparison was made between the proposed muscle control algorithm and simple application of knee torques. Comparing the proposed control to the simple torque application, there was a 41% smaller root-mean-square deviation for a 200N muscle force and a 13% smaller root-mean-square deviation for a 550N desired muscle force in the benchmark test.

Potential future work includes creating a wearable design versus the current mounted design to promote marketability and functionality, and discussions with physical therapists to determine desired muscle force profiles and efficient muscle exercises for patients. Note that the proposed muscle control is not necessarily limited to constant force generation. Any non-constant force profiles may be used. For example, this would enable future robotic gait training that applies a specific resistance to a target muscle. The technical issues discussed in the discussion section should be addressed in the future work.

Acknowledgements

The first author would like to thank the Science, Mathematics, And Research for Transformation Scholarship (SMART) for funding this research. This work was supported in part by National Science Foundation Grant IIS 1142438. The authors would like to thank Dr. Minoru Shinohara for his valuable discussion on this research.

List of symbols and abbreviations

<i>Symbol</i>	<i>Meaning</i>
A	Muscle moment arm matrix
A_a	Cross-sectional area of chamber side “a” of pneumatic actuator
A_b	Cross-sectional area of chamber side “b” of pneumatic actuator
A_{rod}	Cross-sectional area of piston rod of pneumatic actuator
A_{SPOOL}	Area of the spool valve
B	Pneumatic actuator to knee moment arm matrix
c_i	Weighting factor for the i -th muscle in the minimization function
e	Joint torque error in the iterative method
F	Pneumatic actuator force vector
F_{Actual}	Actual force generated by actuator
$F_{Friction}$	Cylinder friction force
F_K	Reference pneumatic actuator force to knee joint

\mathbf{f}	Muscle force vector
f_i	Muscle force of the i -th muscle
f_{id}	Desired Muscle force of the i -th muscle
\hat{f}_i	Predicted Muscle force of the i -th muscle
f_{MAXi}	Maximum contracting force of muscle of the i -th muscle
\mathbf{g}	Gravity vector
i	i -th muscle
j	Number of physical joints
K_I	Integral gain of pressure PI controller
K_P	Proportional gain of pressure PI controller
K_{Loop}	Update value in the iterative method
M_A	Muscle Torque about the ankle joint
M_H	Muscle Torque about the hip joint
M_K	Muscle Torque about the knee joint
m_a, \dot{m}_a	Mass / change in mass of air in chamber side “a” of actuator
m_b, \dot{m}_b	Mass / change in mass of air in chamber side “b” of actuator
N	Number of subjects in the study
n	Number of muscles defined
$PCSA_i$	Physiological cross sectional area of the i -th muscle
P_a	Pressure within chamber side “a” of pneumatic actuator
\dot{P}_a	Change in pressure within chamber side “a” of actuator
P_{atm}	Atmospheric pressure
P_b	Pressure within chamber side “b” of pneumatic actuator
\dot{P}_b	Change in pressure within chamber side “b” of actuator
r	Integer number
s	Laplace – General Purpose Complex Variable
T	Transposed
$u(\mathbf{f})$	Cost (minimization) function
ε	Specified threshold for torque error in the iterative method
α	Value <1 to slowly make K_{Loop} smaller after each iteration
θ_A	Angle of ankle (radians)
θ_H	Angle of knee (radians)
θ_K	Angle of hip (radians)
σ_{MUSCLE}	Specific muscle strength
τ	Time constant of pneumatic cylinder
$\boldsymbol{\tau}_{ACTUATOR}$	Pneumatic actuator torque vector
$\boldsymbol{\tau}_{MUSCLE}$	Torques generated by muscles in vector
τ_A	Actuator Torque at the ankle joint
τ_H	Actuator Torque at the hip joint
τ_K	Actuator Torque at the knee joint

Biography

Gregory C. Henderson received his B.S. and M.S. degrees in Mechanical Engineering from Pennsylvania State University and Georgia Institute of Technology respectively. Since graduating in 2012, he started working on RADAR systems for the United States Army as a Mechanical Engineer.

Jun Ueda received the B.S., M.S., and Ph.D. degrees from Kyoto University, Kyoto, Japan, in 1994, 1996, and 2002 all in Mechanical Engineering. He was an Assistant Professor of Nara Institute of Science and Technology, Japan, from 2002 to 2008. During 2005-2008, he was a visiting scholar and lecturer in the Department of Mechanical Engineering, Massachusetts Institute of Technology. He is currently with the Woodruff School of Mechanical Engineering at the Georgia Institute of Technology as an Associate Professor. He received a Fanuc FA Robot Foundation Best Paper Award in 2005. He is a co-recipient of the 2009 IEEE Robotics and Automation Society Early Academic Career Award.

References

- [1] J. Ueda, D. Ming, V. Krishnamoorthy, M. Shinohara, and T. Ogasawara., "Individual Muscle Control using an Exoskeleton Robot for Muscle Function Testing," *IEEE Transactions on Neural Systems and Rehabilitation Engineering*. Vol. 18, 339-350, (Aug. 2010).
- [2] R. Riener and T. Fuhr, "Patient-driven control of FES supported standing-up: a simulation study," *IEEE Trans. Rehab. Eng.*, Vol. 6, pp.113–124, (June 1998).
- [3] S.J. Piazza, S.L. Delp. "The influence of muscles on knee flexion during the swing phase of gait," *Journal of Biomechanics* 29,723–733. (1996).
- [4] X. Shen, and M. Goldfarb. "Simultaneous Force and Stiffness Control of a Pneumatic Actuator," *Journal of Dynamic Systems, Measurement, and Control*. Vol. 129, 425-434, (July 2007).
- [5] Fujita, T., Kawashima, K., and Kagawa, T. "Effect of servo valve dynamic on precise position control of a pneumatic servo table," *International Journal of Automation Technology* 2.1, 43-48.(2008).
- [6] Andersson, S., Soderberg, A., and Bjorklund, S., "Friction models for sliding dry, boundary and mixed lubricated contacts," *Tribology International*. Vol. 40, no. 4, pp. 580-587, (2007).
- [7] Shu, N. and Bone, G.M., "Development of a nonlinear dynamic model for a servo pneumatic positioning system," in *Mechatronics and Automation, 2005 IEEE International Conference*, vol. 1, 00. 43-48 Vol. 1, (2005).
- [8] Zhu, Y. and Barth, E.J., "Impedance control of a pneumatic actuator for contact tasks," in *2005 IEEE International Conference on Robotics and Automation, April 18, 2005 - April 22, 2005*, Vol. 2005, p. 987 – 992, (2005).
- [9] RD. Crowninshield, et al., "A physiologically based criterion of muscle force prediction in locomotion," *J. Biomechanics*, Vol, 14, pp. 793–801, (1981).
- [10] G. Yamaguchi, *Dynamic modeling of musculoskeletal motion*. Kluwer Academic Publishers, (2001).

- [11] B. van Bolhuis and C. Gielen, "A comparison of models explaining muscle activation patterns for isometric contractions," *Biological Cybernetics*, Vol. 81, no. 3, pp. 249–261, (1999).
- [12] Erdemir, A., McLean, S., Herzog, W., van den Bogert, A.J., "Model-based estimation of muscle forces exerted during movements," *Clinical Biomechanics* Vol. 22, 131–154. (2007).
- [13] J. Biggs and K. Horch, "A three-dimensional kinematic model of the human long finger and the muscles that actuate it," *Medical Engineering and Physics*, Vol. 21, no. 9, pp. 625–639, (1999).
- [14] S. Delp, J. Loan, M. Hoy, F. Zajac, E. Topp, J. Rosen, V. Center, and P. Alto, "An interactive graphics-based model of the lower extremity to study orthopaedic surgical procedures," *IEEE Transactions on Biomedical Engineering*, Vol. 37, no. 8, pp. 757–767, (1990).
- [15] W. Maurel and D. Thalmann, "A Case Study on Human Upper Limb Modeling for Dynamic Simulation," *Computer Methods in Biomechanics and Biomedical Engineering*, Vol. 2, no. 1, pp. 65–82, (1999).
- [16] H. Veeger, F. Van der Helm, L. Van der Woude, G. Pronk, and R. Rozendal, "Inertia and muscle contraction parameters for musculoskeletal modeling of the shoulder mechanism," *J Biomech*, Vol. 24, no. 7, pp.615–29, (1991).
- [17] Patriarco, A. B., Mann, R. W., Simon, S. R., and Mansour, J. M., "An Evaluation of the Approaches of Optimization Methods in the Prediction of Muscle Forces During Human Gait," *J. Biomech.*, Vol. 14, pp. 513–525, (1981).
- [18] Raikova, R.T., Prilutsky, B.I., "Sensitivity of predicted muscle force to parameters of the optimization-based human leg model revealed by analytical and numerical analyses," *J. Biomech.* Vol. 34, 1243–1255, (2001).
- [19] Stokes, I.A.F., Gardner-Morse, M., "Lumbar spinal muscle activation synergies predicted by multi-criteria cost function," *Journal of Biomechanics* Vol. 34, 733–740. (2001).
- [20] Infantolino BW, Challis JH. "Architectural properties of the first dorsal interosseous muscle," *Journal of Anatomy*. 216(4):463–469, (2010).
- [21] Kellis E and Baltzopoulos V., "Muscle activation differences between eccentric and concentric isokinetic exercise," *Med Sci Sports Exerc* 30: 1616–1623, (1998).
- [22] Westing, S. H., A. G. Cresswell, and A. Thorstensson., "Muscle activation during maximal voluntary eccentric and concentric knee extension," *Eur. J. Appl. Physiol.* 62:104-108, (1991).
- [23] H. Kazerooni, J.-L. Racine, L. Huang, and R. Steger., "On the control of the Berkeley Lower Extremity Exoskeleton (BLEEX)," *IEEE International Conference on Robotics and Automation*, pages 4353–4360, (April 2005).
- [24] H. Kawamoto, Suwoong Lee, S. Kanbe, and Y. Sankai., "Power assist method for HAL-3 using EMG-based feedback controller," *IEEE International Conference on Systems, Man and Cybernetics*, 2:1648–1653, (2003).
- [25] J. A. Blaya and H. Herr, "Adaptive control of a variable-impedance ankle-foot orthosis to assist drop-foot gait," *IEEE Trans. Neural Syst.Rehabil. Eng.*, Vol. 12, no. 1, pp. 24–31, (Mar. 2004).

- [26] B. Volpe, P. Huerta, J. Zipse, A. Rykman, D. Edwards, L. Dipietro, N. Hogan, and H. Krebs, "Robotic devices as therapeutic and diagnostic tools for stroke recovery," *Arch. Neurol.*, Vol. 66, no. 9, pp. 1086–1086, (2009).
- [27] J. Furusho, M. Sakaguchi, N. Takesue, and K. Koyonagi, "Development of ER brake and its application to force display," *J. Intell. Mater. Syst. Struct.*, Vol. 13, pp. 425–429, (2002).
- [28] Book, W. and Ruis, D., "Control of a robotic exercise machine". In *Proc. of the Joint Automatic Control Conference*, pages WA.2A. (1981).
- [29] Richer E, Hurmuzlu Y., "A high performance pneumatic force actuator system: Part I-Nonlinear mathematical model." *ASME J Dyn Syst Meas Control*. Vol. 122:416–425. (2000).
- [30] Kamper DG, Fischer HC, Cruz EG., "Impact of finger posture on mapping from muscle activation to joint torque," *Clin Biomech* 21: 361–369, (2006).
- [31] A. D. Deshpande, R. Balasubramanian, R. Lin, B. Dellon, and Y. Matsuoka, "Understanding variable moment arms for the index finger MCP joints through the ACT hand," *IEEE Conference on Biomedical Robotics and Biomechatronics*, pp. 776-782 (2008).
- [32] T. S. Buchanan, D. G. Lloyd, K. Manal, and T.F. Besier, "Neuromusculoskeletal modeling: Estimation of muscle forces and joint moments and movements from measurements of neural command," *J. Appl. Biomech.*, Vol. 20, pp. 367-395, (2004).
- [33] Cheng AJ, Rice CL, "Fatigue and recovery of power and isometric torque following isotonic knee extensions," *J Appl Physiol.*, Vol. 99: 1446–1452, (2005).
- [34] Knapik, J. J., Wright, J. E., Mawdsley, R. H., et al. "Isometric, isotonic, and isokinetic torque variations in four muscle groups through a range of joint motion." *Physical Therapy*, 63, 938-947, (1983).
- [35] Jun Ueda and Ming Ding, "Individual Control of Redundant Skeletal Muscles using an Exoskeleton Robot," *Redundancy in Robot Manipulators and Multi-Robot Systems*, Lecture Notes in Electrical Engineering, pp. 183-199, Vol. 57, Edited by Dejan Milutinovic and Jacob Rosen, ISBN 978-3-642-33970-7, Springer, (2013).
- [36] Gregory Henderson, "Pneumatically-Powered Robotic Exoskeleton to Exercise Specific Lower Extremity Muscle Groups in Humans," Masters Thesis, Georgia Institute of Technology, (2012).
- [37] Hidler, Joseph and Nichols, Diane and Pelliccio, Marlena and Brady, Kathy and Campbell, Donielle D and Kahn, Jennifer H and Hornby, T George, "Multicenter randomized clinical trial evaluating the effectiveness of the Lokomat in subacute stroke," *Neurorehabilitation and Neural Repair*, Vol. 23, no. 1, 5-13, (2009).
- [38] Delp, S., Anderson, F., Arnold, A., Loan, P., Habib, A., John, C., Guendelman, E., Thelen, D, "Opensim: open-source software to create and analyze dynamic simulations of movement," *IEEE Transactions on Biomedical Engineering* ,54(11), 1940–1950, (2007).
- [39] Damsgaard, M., Rasmussen, J., Christensen, S., Surma, E., de Zee, M, "Analysis of musculoskeletal systems in the ANYBODY modeling system," *Simulation Modelling Practice and Theory* 14(8), 1100–1111, (2006).
- [40] KM Steele, A Seth, JL Hicks, M Schwartz, SL Delp, "Muscle contributions to support during single-limb stance in crouch gait." *Journal of Biomechanics*, Vol. 43, 2099-105, (2010).

- [41] Weir, J.P, Wagner, L.L., & Housh, T.J, “Linearity and reliability of the IEMG v. torque relationship for the forearm flexors and leg extensors,” *American Journal of Physical Medicine and Rehabilitation*, Vol. 71, 283-287, (1992).
- [42] Anderson, F.C., and Pandy M. G., “Dynamic Optimization of Human Walking,” *Journal of Biomechanical Engineering*, Vol. 123, 381-390, (2001).
- [43] MotCo project, <http://www.clbme.bas.bg/projects/motco/>
- [44] Ellenor Brown, Kazuya Aomoto, Atsutoshi Ikeda, Tsukasa Ogasawara, Yasuhide Yoshitake, Minoru Shinohara, Jun Ueda, "Comparison of Ultrasound uscle Stiffness Measurement and Electromyography towards Validation of An Algorithm for Individual Muscle Control," *2013 ASME Dynamic Systems and Control Conference (DSCC'13)* in CD-ROM, (2013).
- [45] Noritsugu, T., and Takaiwa. M., “Robust positioning control of pneumatic servo system with pressure control loop,” *Proceedings of 1995 IEEE International Conference on Robotics and Automation*. Vol. 3, pp. 2613-2618, (1995).